Electronic Supplementary Information

Harnessing combinational phototherapy via post-synthetic PpIX conjugation on nanoscale metal-organic frameworks

*Rui Chen, Wen-Cheng Chen, Li Yan, Shuang Tian, Bin Liu, Xianfeng Chen, Chun-Sing Lee, and Wenjun Zhang**

Dr. R. Chen, Dr. L. Yan, Dr. B. Liu, Prof. W. Zhang
Center of Super-Diamond and Advanced Films (COSDAF), Department of Materials Science and Engineering, City University of Hong Kong, Hong Kong SAR, P. R. China
E-mail: apwjzh@cityu.edu.hk
Dr. W-C. Chen, S. Tian, Prof. C.-S. Lee
Center of Super-Diamond and Advanced Films (COSDAF), Department of Chemistry, City University of Hong Kong, Hong Kong SAR, P. R. China
Dr. X. Chen
School of Engineering, Institute for Bioengineering, The University of Edinburgh, King's Buildings, Mayfield Road, Edinburgh EH9 3JL, UK

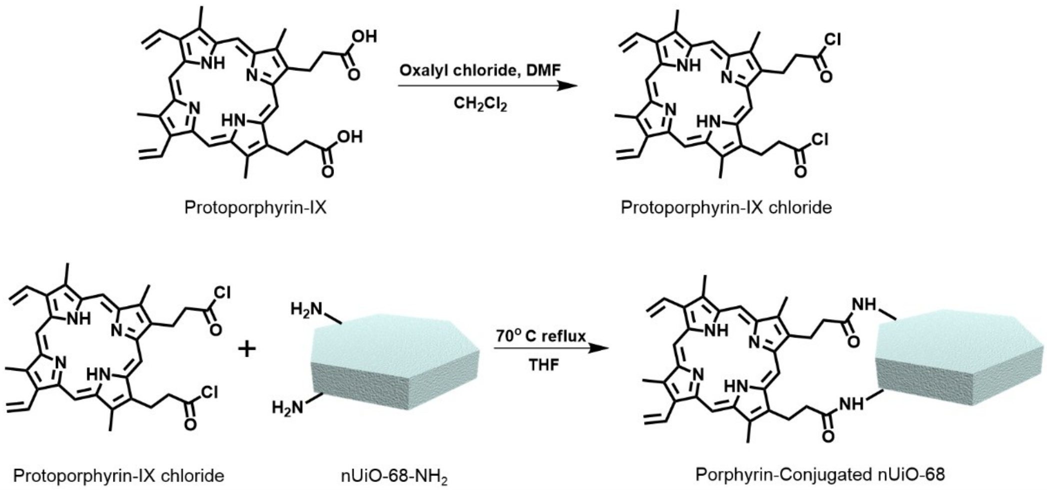

Scheme S1 Synthetic route of PpIX chloride and nPCU NPs.

Table S1 Reactant ratios of PpIX and NMOFs, conjugation efficiency and content of PpIX in nPCU NPs.

nPCU NPs	1	2	3	4	5	6
PpIX:NMOF (μmol:mg)	0.04	0.08	0.2	0.4	0.8	1
Efficiency[a] /%	100	100	100	97.3	86.2	72.9
Content[a] /wt%	2.2	4.3	10.1	18.0	28.0	29.1

[a]Conjugation efficiency and content are calculated as described in the supplementary section preparation of nPCU NPs.

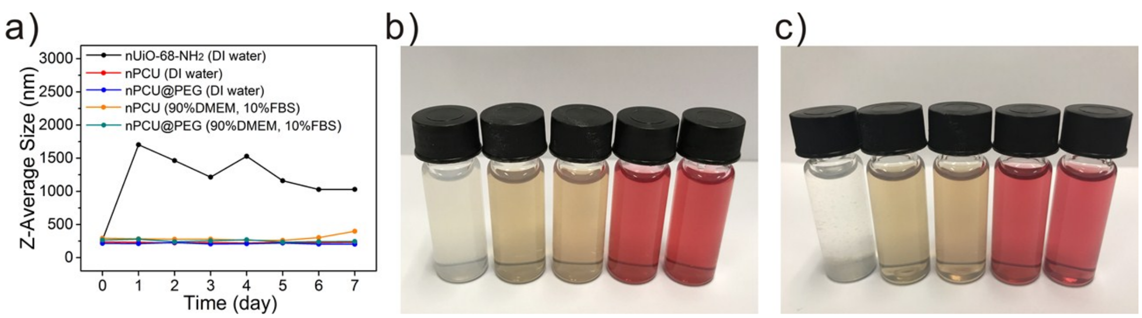

Fig. S1. a) Size stability of nUiO-68-NH_2, nPCU, nPCU@PEG NPs in water, and nPCU, nPCU@PEG NPs in 90% DMEM associated with 10% FBS (cell medium). Photographs of b) freshly dispersed NPs solutions and c) those after 7 days without any perturbation. From left to right: nUiO-68-NH_2 in water, nPCU in water, nPCU@PEG in water, nPCU in cell medium, nPCU@PEG in cell medium.

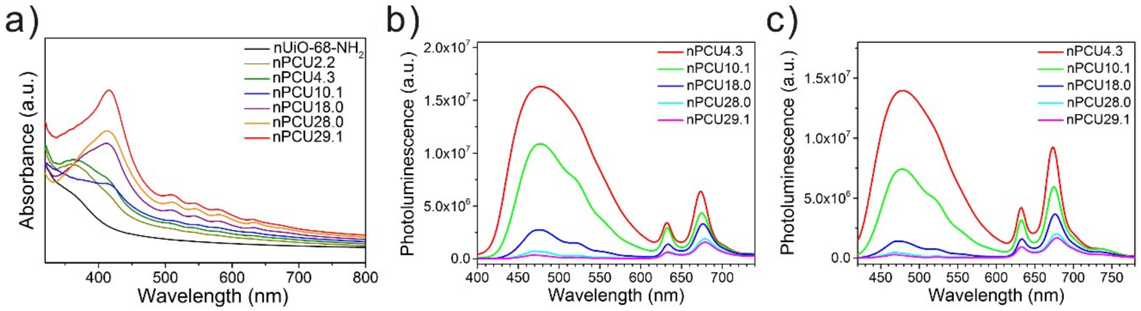

Fig. S2 (a) Absorption and photoluminescence spectra of nPCUx NPs excited at b) 380 nm and c) 400 nm.

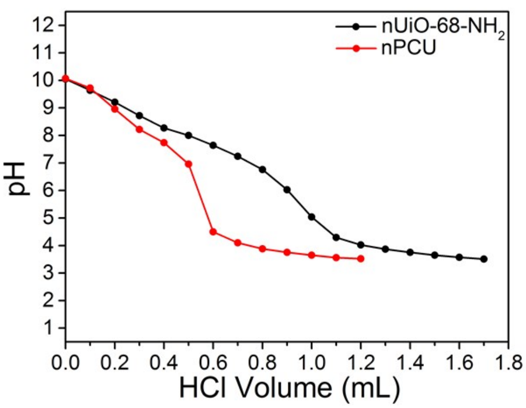

Fig. S3 Acid titration profiles of 0.2 mg/mL nUiO-68-NH_2 and nPCU NP in 20 mL aqueous solutions. The pH value of the solutions were adjusted to 10 using 0.06 M NaOH aq., and titrated with 0.01 M HCl aq. to reach 3.0.

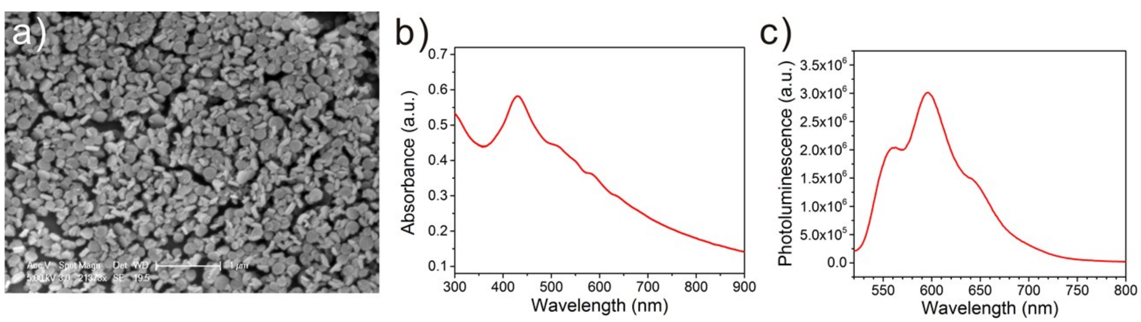

Fig. S4 a) SEM image, b) UV-vis absorption spectrum, and c) fluorescence spectrum of DOX-loaded nPCU (nPCU/DOX) NPs.

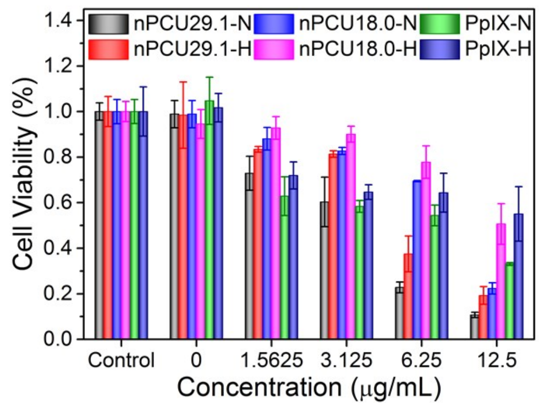

Fig. S5 *In vitro* phototherapy of A549 cells incubated with PpIX, nPCU18.0 and nPCU29.1 NPs in normoxic and hypoxic conditions, followed by 635-nm laser irradiation (100 mW/cm^2, 3 min).

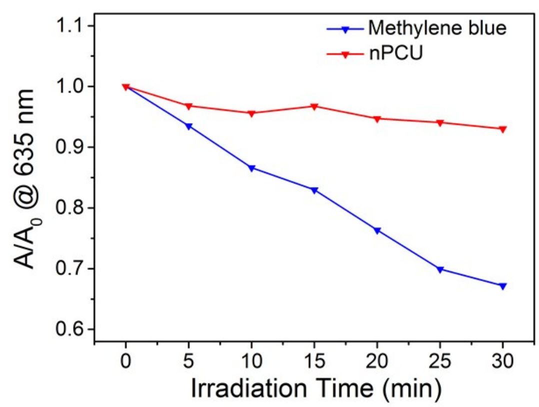

Fig. S6 Relative absorption value at 635 nm of nPCU NPs and methylene blue in dependence of laser irradiation time.

Fig. S7 Photographs of nUiO-68-NH_2/PpIX (left) and nPCU (right) solutions.

Direct immersing NMOFs in drug solution generally renders very low loading capacity and burst-release kinetics because the delivery process relies on physical molecule diffusion and host-guest interaction. With respect to phototherapy, photoactive nanomaterials need to localize at tumor sites with high stability. Therefore, PpIX is preferred to be grafted to the amines of NMOFs to construct stable phototherapeutics.

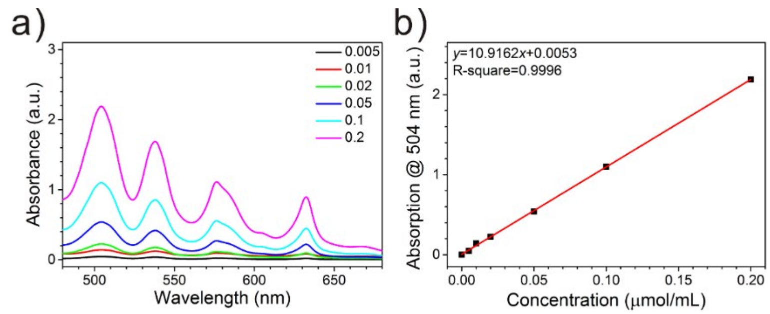

Fig. S8 (a) Absorption spectra of PpIX chloride with different concentrations. (b) Standard correlation curve of absorption peak versus concentrations of PpIX chloride.

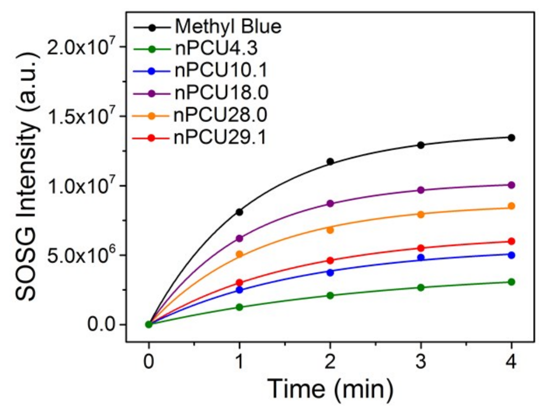

Fig. S9 Singlet oxygen generation of methylene blue and nPCUx NPs, evaluated by fluorescence increase of SOSG.

Table S2 Fitting parameters of singlet oxygen generation efficiency.

	Methylene blue	nPCU4.3	nPCU10.1	nPCU18.0	nPCU28.0	nPCU29.1
$A(10^6)$	13.89	3.90	5.64	10.32	8.73	6.54
$k(min^{-1})$	0.89	0.39	0.58	0.92	0.82	0.62
Ak	12.36	1.52	3.27	9.49	7.16	4.05
Efficiency[a]	1	0.12	0.26	0.77	0.58	0.33

[a]Efficiency is calculated via normalizing Ak of different samples by that of methylene blue.

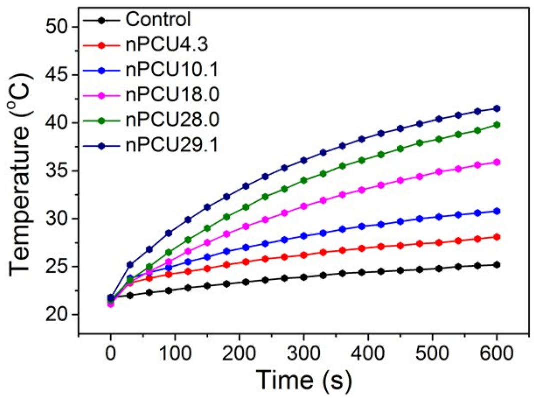

Fig. S10 Temperature elevation of nPCUx NPs in water with extending irradiation time of 635-nm laser at 1 W/cm^2.

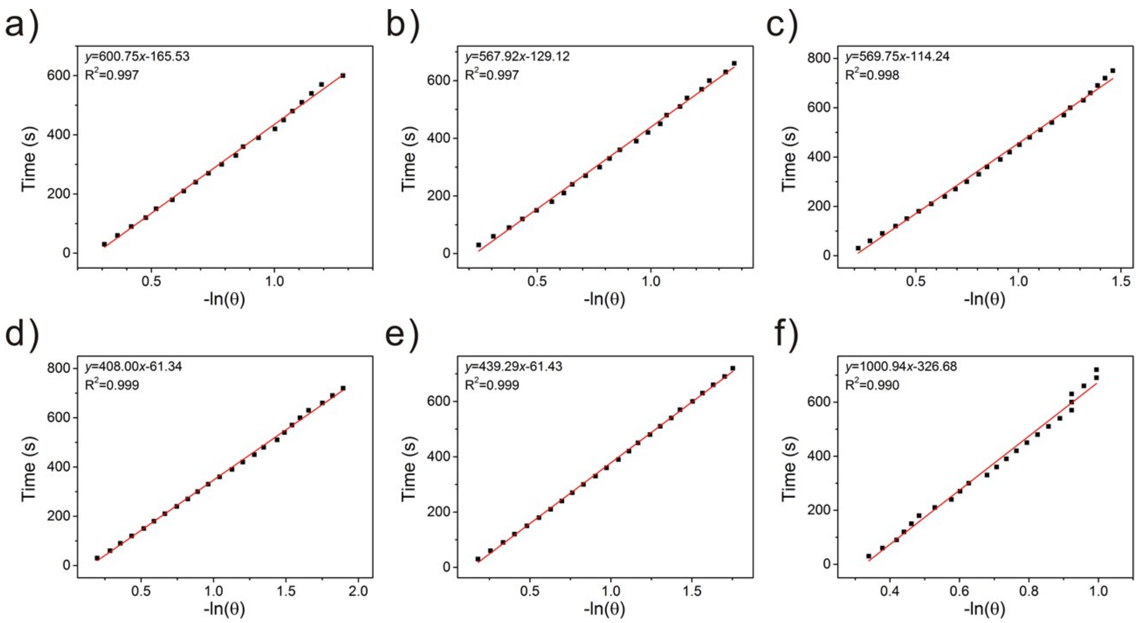

Fig. S11 Photo-thermal conversion efficiency calculation of nPCU4.3, 10.1, 18.0, 28.0, 28.1 and water.

The heating and cooling curves of nPCUx under laser irradiation were collected to compute their photo-thermal conversion efficiencies.

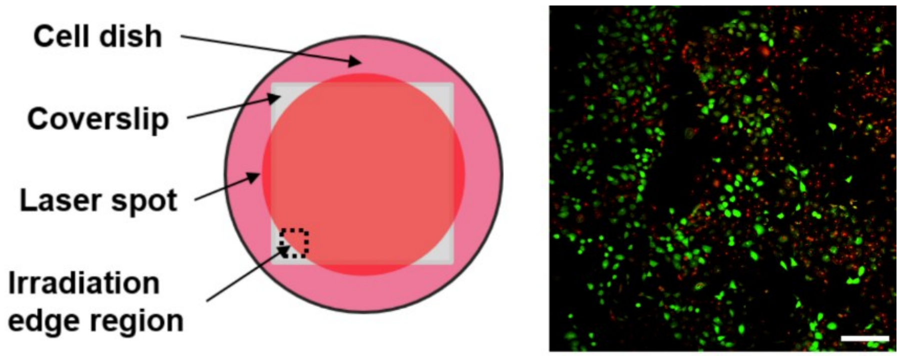

Fig. S12 CLSM images of A549 cells at edge region of laser spot. The cells were treated with nPCU NPs and irradiation, followed by calcein-AM and PI co-staining.

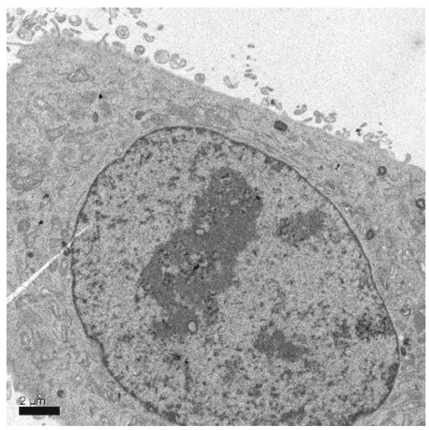

Fig. S13 TEM image of an A549 cell.

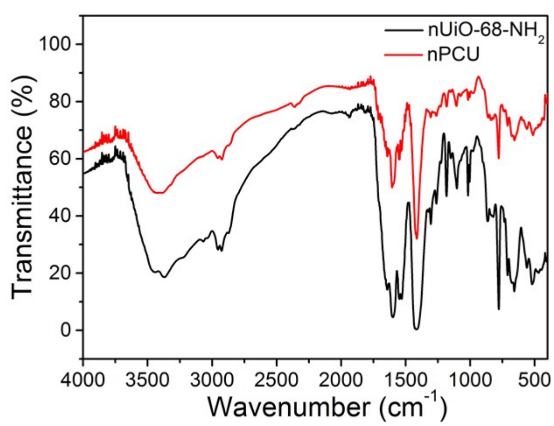

Fig. S14 Fourier transform infrared spectroscopy of nUiO-68-NH_2 and nPCU NPs. In 3475-3350 cm^{-1}, nUiO-68-NH_2 shows two N-H stretch bands of primary amines. Whereas, there is only one N-H stretch band in nPCU, indicating the existence of secondary amide ascribed to PpIX conjugation.